Pol. J. Environ. Stud. Vol. 34, No. 2 (2025), 1733-1743
DOI: *10.15244/pjoes/188064* ONLINE PUBLICATION DATE: 2024-08-05

Original Research

Mapping and Monitoring of Landforms Evolution. Case study: Breasta Landslide (Southwestern Romania)

Daniel Simulescu[1, 2], Oana Mititelu-Ionuș[1], Sandu Boengiu[1], Valentina Nikolova[3], Cristiana Vîlcea[1], Mirela Mazilu[1], Simona Mariana Popescu[4*], Emil Marinescu[1]

[1]Department of Geography, Faculty of Sciences, University of Craiova, 13 A.I Cuza, 200585, Craiova, Romania
[2]Dolj Territorial Service, National Agency for Protected Natural Areas, Craiova, Romania
[3]Department of Geology and Geoinformatics, University of Mining and Geology, Sofia, Bulgaria
[4]Department of Biology and Environmental Engineering, Faculty of Horticulture, University of Craiova, 13 A.I Cuza, 200585, Craiova, Romania

Received: 25 December 2023
Accepted: 27 April 2024

Abstract

The steep right slope of the Jiu River (a tributary of the Danube River in the Romanian Plain) in its lower course is one of the hotspots for landslides in Southwestern Romania, constantly facing instability issues due to landslide reactivations and slope-related active deformations. In our study, we aimed to analyze the behavior of the Breasta landslide. The 16-year monitoring data set (2006-2022) contributes to a better understanding of the movement mechanisms associated with triggering factors. Following GNSS monitoring of the profile line since 2006, it became obvious that the most significant morphological changes occurred in the median and final sectors of the landslide, where the slope retreated by 6 to 19 meters. In terms of results, a digital terrain model of the central sector of the Breasta landslide was generated using 5000 GPS-measured points. Using the Kriging method, this sector was enclosed within a rectangle covering an area of 313.40 square meters, with an average height of 108 meters. This sector emphasizes the morphology of the landslide from 2022 in one of the 'amphitheaters' that developed after the 2006 reactivation. This paper provides insights into the dynamics of the landslide, helping to discover possible triggering factors of mass movement and periodic changes in the landslide morphology.

Keywords: landslide, mass movement, GNSS measurements, GIS, surface analysis, Southwestern Romania

*e-mail: simona.popescu@edu.ucv.ro

Introduction

Landslides are one of the most common and destructive natural hazards [1]. Actually, a landslide is a complex phenomenon [2] that is caused mainly by natural conditions. The activation factors in landslide-prone areas, like the effects of water (through massive precipitation and snowmelt) or seismic activity, may have an instantaneous effect with devastating consequences [3].

Studies of landslide evolution that improve the knowledge of ground movements are essential to understanding the deformation mechanism [4] and mapping the associated risk. In this regard, consistent monitoring of mass movement events is needed for a reliable hazard and risk assessment, as well as to mitigate their devastating effects.

Numerous landslide studies show that the monitoring systems are designed to primarily satisfy two purposes: understanding the extension of the phenomenon [5] or providing early warnings, even defining the time of failure [6], and identifying the variation and dynamics of landslides in real time [7]. Monitoring, rate, location, and displacement vector often represent the most effective methods for defining landslide behavior, allowing users to observe reactivation due to external triggering factors and to assess the effectiveness of mitigation measures [8, 9].

Landslide susceptibility analysis can be considered the first stage of hazard assessment. It generally follows two approaches: quantitative and qualitative, with the latter being a concern for experts and feasible only on a local scale [10]. The quantitative approach is the best practice, and it can be divided into two parts: statistical models and physically based models [11]. Statistical models require historical data on slope failures, which does not consider the failure mechanism [12] and also ignores temporal fluctuations of groundwater level. Physically-based models estimate slope instability by measuring geometrical and geotechnical parameters and are an excellent approach for monitoring shallow landslides [13]. They also generally follow a grid-based structure, making them convenient for GIS environments with input raster files including information on soil properties, vegetation, elevation, and rainfall [14, 15].

Consequently, reliable landslide susceptibility analysis results are vital for policymakers to manage regional-scale landslide risk [10]. In recent studies, landslide risk management requires greater leveraging of big data, more strategic use of monitoring resources, and better communication with residents [16, 17].

This paper provides insights into the dynamics of the Breasta landslide, helping to discover the mass movement and its deformations as the result of periodic changes. The main aim of landslide mapping and monitoring is to value the triggering factors' contribution to landslide reactivation. In this regard, the research stages are as follows:

– Field measurements of the reactivated part of the landslide using GPS
– Correlation of the mass movement measurements with the quantity of rainfall, groundwater, and surface water levels and pressures
– Evaluation of the input data using GIS tools
– Obtaining a landslide deformation model based on combining all of the existing data

Material and Methods

Study Area

In Romania, landslide occurrence (in terms of first-time failures or subsequent reactivations) is determined by predisposing, preparing, and triggering factors, each with a different and particular share; the most common one is exceptionally heavy rainfall, which exceeds the levels normally encountered in the area where landslides occur [18, 19]. Recent studies have shown quite some progress in understanding landslide dynamics at different scales [20-23].

Regarding landslide assessment, some researchers consider physiographic and climatic elements to be significant factors that influence regional characteristics in the interaction of landslide conditioning factors [22]. In the case of the Breasta landslide, the fluctuation of water levels, in combination with the lithological composition, influences the deformation and failure processes. Therefore, an analysis of the temporal and spatial evolution of the Breasta landslide under the influence of rainfall conditions can offer valuable insights and recommendations for disaster prevention and reduction. Within the lower Jiu River sector, the paleogeographic evolution led to the formation of a morpho-hydrographic corridor. The erosion of Piedmontan structures and the development of a terraced plain occurred during the climatic fluctuations of the Pleistocene and neotectonic movements, resulting in the deviation of the Danube towards the right and the lowering of its base level [24].

The Jiu River has repeatedly altered its course within the floodplain. The continuous erosion of the right bank of the Jiu River and its Romanian-Pleistocene deposits, composed of a mixture of clays, marls, and sands, has resulted in the preservation of a steep slope with an angle exceeding 65°, making it highly susceptible to landslides. The river generally follows its course along the right bank, veering away only at confluence points and downstream from its tributaries, which have deposited alluvial fans in the floodplain. Among the numerous landslides in the lower course of the Jiu River, the most significant ones are located near Bâlta, Breasta (see Fig. 1), Bucovăţ, Bâzdâna, and Drănic localities.

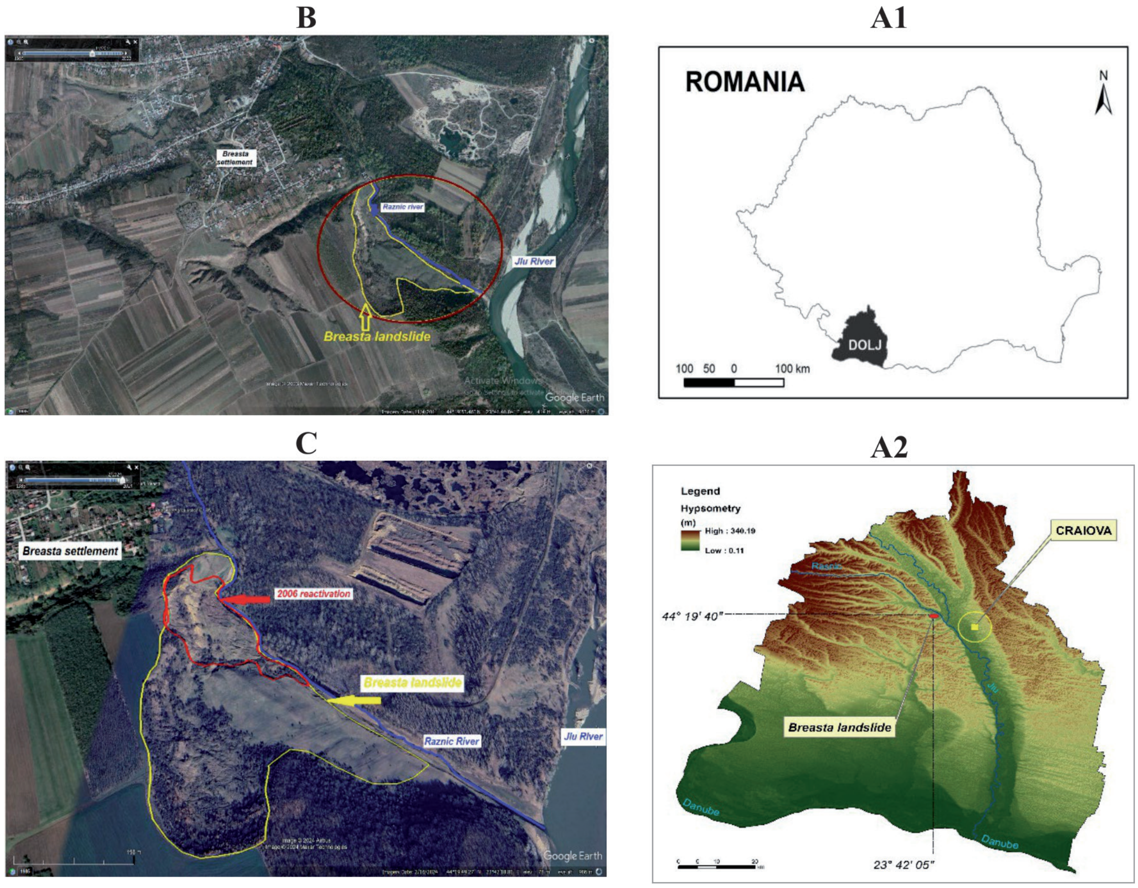

Fig. 1. Study area location – A (A1 – national scale; A2 – regional scale); Breasta landslide extension (local scale) - B (Google Earth PRO, November 2011); Breasta landslide extension (local scale) - C (Google Earth PRO, November 2021).

Methodological Inputs

Methods such as field observation and real-time monitoring are widely used to study the deformation characteristics and triggering mechanisms of landslides [25-27]. GNSS control networks were built to monitor landslide deformation and acquire landslide displacement time series. Topographic data calculation is the key for several geomorphic applications, especially landform monitoring and evolution [28].

The concept of monitoring landslides with GPS technology has been demonstrated in numerous studies [28-30]. For GPS measurements, at least five satellites are needed. The landslide spatial datasets can be established using GIS spatial interpolation, superposition analysis, and other functions [31]. Spatial resolutions are proportional to the landform size that can be mapped, as well as the research scope [32]. From the wide variety of software packages for preparing, digitizing, editing, and presenting digital cartography, we used in our research the ESRI ArcGIS software in its ArcMap environment. The applications included in the Spatial Analyst toolbox (Interpolation toolset) and 3D Analyst toolbox (Raster Interpolation toolset) allowed us to interpolate values between sample locations and generate a raster format [33].

Breasta landslide data were updated based on photo interpretation of high-resolution satellite images (dating from 2006 to 2021) available on the Google Earth platform by digitizing polygons at a scale of 1:5,000. Additionally, the methodology used in this research is presented in Fig. 2.

Digital Surface Analysis and Landslide Mapping

Geomorphological maps play a crucial role in illustrating the distribution of landforms and the processes related to their geomorphic environments [34, 35]. To manage this data effectively, GIS software packages provide a variety of tools for visualizing, manipulating, and analyzing extensive GPS data [36].

A surface model is composed of a series of surfaces and can be categorized into two types: a Triangular Irregular Network (TIN) and a regular square grid (grid). A TIN model represents the land surface using vectors, comprising irregularly spaced nodes and lines with three-dimensional coordinates, organized into a network of non-overlapping triangles. Over a span of 16 years (2006-2022), 30 repeated GNSS field observations and surveys were conducted to assess the activity of the landslide and understand its kinematic behavior. For measurements, we used the GNSS receiver

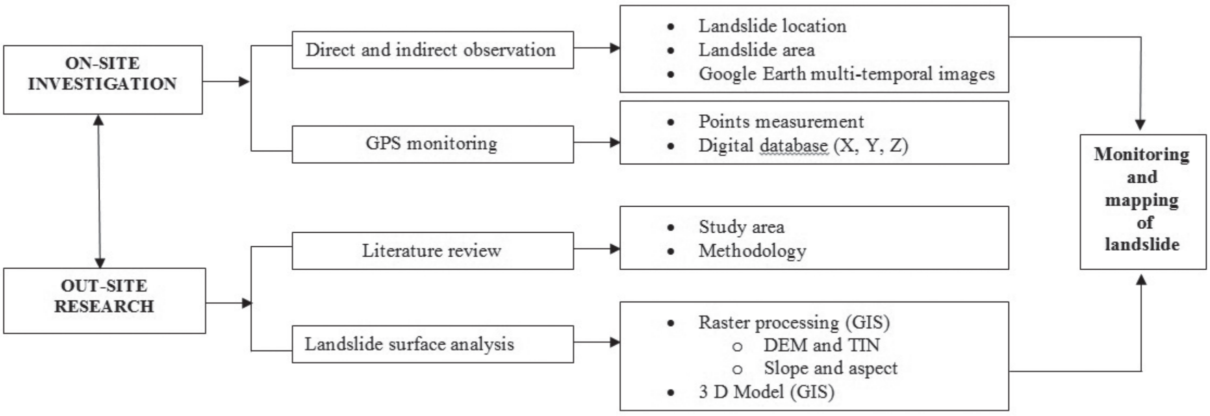

Fig. 2. Methodological flowchart used in the assessment of Breasta landslide.

SOUTH S82-T, which converts signals from visible satellites (such as GPS, GLONASS, GALILEO, SBAS, and Compass) into positions on Earth. The receiver was connected simultaneously to ROMPOS (Romanian Position Determination System), which provides real-time positioning services, including differential corrections for real-time kinematic positioning (RTK). This service allows access to the Network RTK product, which calculates corrections based on observations from the nearest reference stations around the user. For any measurements performed using GNSS technology, the coordinates obtained are by default in the WGS84 reference and coordinate system. By connecting the receiver to ROMPOS reference stations, in the case of real-time measurements, the resulting coordinates for the new points will be taken in the ETRS89 system. The results indicate the difficulty in predicting Breasta landslide displacement due to the highly non-linear and non-stationary characteristics present in the time series of displacement. The topographical slope of the Breasta landslide was derived using GIS software, which enabled the creation of an estimated slope map based on contours from shaded relief. The collected data facilitated the creation of a precise map of the Breasta landslide (refer to Fig. 3).

Comparative analysis of the obtained Digital Terrain Models (DTMs) also allowed the identification of areas of the slope prone to failure and the assessment of the extent of the mass involved [37]. From various interpolation techniques, we selected the Kriging option for surface creation, as it is highly effective when there is a high degree of spatial autocorrelation and a clear directional pattern in the dataset. To obtain clear results, the Digital Terrain Models (DTMs) were visualized using the Arc Scene extension without exaggeration of the vertical scale, known as Base Heights. This visualization method aided in identifying recent scarps, which were correlated with field measurement data for the characteristics of the landslide surface, such as slope and aspect. In addition, changes within the landslide area between 2006 and 2022 were identified in an ArcGIS environment by estimating the slope derived from the DTM. To obtain clear results, the resulting DTMs were visualized using the Arc Scene extension without exaggeration of the vertical scale (Base Heights), which was helpful in detecting recent scarps correlated with field measurement data.

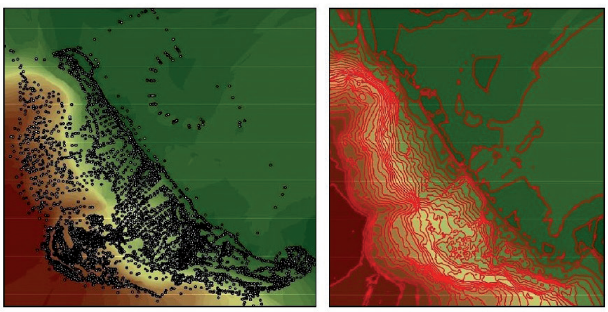

Fig. 3. Highlight of GPS measurement points (left); lines, generated of the point data (right).

Results and Discussion

Triggering Factors Identified

In the lower basin, the Jiu River has consistently undercut the right slope of the valley. This is attributed to major Quaternary events, such as the Jiu's tendency to deviate westward due to variations in topographic elevation speeds, which are higher in the east and lower in the south, as recorded in the western regions of the Moesian Plate. The encountered structures consist of homocline landforms, from northwest to southeast, in the Getic Piedmont and tabular structures in the Romanian Plain. From the lithological perspective, they are composed of sedimentary complexes formed by loosely cemented sands and gravels alternating with marl and clays. During the Middle Pleistocene, in the southwest of Romania, an upheaval movement began that is still active today. This general upheaval process was accompanied by folds resulting from the local differentiation of relief forms, the intensification and development of slope processes, and changes in riverbed lithology.

The effect of these movements varied depending on the existing faults, with uneven upheaval in different areas of the Getic Platform leading to accentuated erosion. In most cases, the Jiu River moves away from the right slope near the confluences with its right tributaries, but later returns near the slope. This is a result of the Piedmont homocline tilting from northwest to southeast, thus causing all landslides to occur accordingly. They unfold in a common mechanism, which is synchronized with increased rainfall and higher flows of the Jiu River. Geomorphological mapping has revealed numerous cracks, fissures, and micro-depressions where water accumulates. Moreover, it has become evident that various lines of landslide scarps and steps continuously evolve at a microform level. Torrential valleys and gullies with steep slopes were identified as causes of local landslides as they cut through sand levels, triggering the dynamic evacuation of water from divided sand lenses. Depending on the frequency, intensity, quantity, and timing of rainfall, they directly influence soil moisture and vegetation. Climatic conditions, particularly the temperature regime (with an average annual temperature of 11.1ºC), indirectly influence gravitational processes [38]. Higher temperatures and lower precipitation levels facilitate the development of cracks and fissures, allowing water to penetrate deep into the soil [39]. The first major movement of the Breasta landslide occurred in 1940 when, in conjunction with the undercutting of the slope by the Jiu River, an earthquake in Vrancea County (measuring 7.4 on the Richter scale) triggered the Breasta landslide. In 1971, following heavy rainfall, the landslide expanded, adding the second sector [24]. In 2006, the third sector was activated due to substantial precipitation that led to the sliding of the slopes of a gully located upstream, blocking its normal drainage and redirecting groundwater.

Geological data were collected through exploratory coal drilling, hydrogeological drilling, and natural outcrops, as well as excavations made for sampling construction materials (see Fig. 4). The analysis of rainfall data (with a multi-annual mean of 594.3 mm) indicates significant variability in precipitation. Average monthly rainfall varies from 41.3 mm in February to 86.8 mm in June, with an overall average of 59.0 mm per month. Rainy years alternate with drought periods. Median precipitation values recorded between 2005 and 2021 are generally lower than the mean values, indicating a right-skewed distribution for most months (see Fig. 5). The standard deviations reveal considerable variation in rainfall amounts, with the largest standard deviation of 46.8 mm occurring in August. The minimum and maximum values for each month illustrate a wide range of rainfall variability across the years. For example, the minimum rainfall for March is 0 mm, while the maximum is 144.0 mm. Similarly, the minimum rainfall

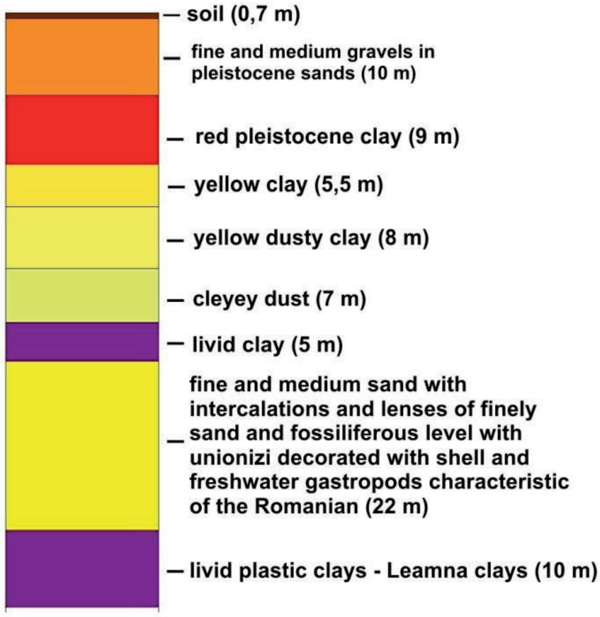

Fig. 4. The lithological profile at Breasta.

for July is 5.6 mm, while the maximum is 170.1 mm (see Table 1). Additionally, between 1991 and 2006, there were significant fluctuations in the precipitation regime (in 1992, there were only 293.5 mm of rainfall, while in 2005, it reached 1081.1 mm, a difference of 788.3 mm) [38]. The graph below shows that in 2005, the highest amount of precipitation (215.8 mm) was recorded in August, along with the second-highest annual average rainfall (90.2 mm). These heavy rainfalls occurred in the year before the 2006 landslide, when the same month had only 143.9 mm of precipitation (see Fig. 5). The monthly rainfall data were taken from the Craiova meteorological station for the period 2005-2021, which is the closest station to the study area.

Landslide Analysis

In 2006, we began monitoring the reactivation of the Breasta landslide by conducting field measurements to highlight its stage and trend of evolution. Field investigations, monitoring, and theoretical analyses were carried out. In total, 30 monitoring campaigns were completed (starting with spring 2006 and ending with autumn 2022). In general, the outings in the field were correlated with the periods in which the amount of precipitation in 24 recorded significant values (August 2006 and 2007; September 2014 and 2015; July 2018 and June 2019). The 3D model of the landslide was created following the measurement campaign in the spring of 2011 (see Fig. 6 and 7).

The Breasta landslide occurred as a result of intensified erosion along the Jiu River's bank during years of excessive rainfall (see Fig. 8). It is a sliding landslide with rotational movements at its bottom. In the microrelief, 2-3 sliding steps and a frontal wave are separated. The detachment scarp is high (up to 8 m),

Table 1. The characteristic values of monthly rainfall data at Craiova meteorological station during 2005-2021.

Month	Mean	Median	Standard Deviation	Min	Max
Jan	53.2	40.3	29.9	4.3	109.9
Feb	41.3	35.6	25.8	4.5	81.6
Mar	58.5	43.5	28.2	8.1	144.0
Apr	45.4	50.0	27.8	0	123.8
May	74.3	66.6	36.1	31.0	153.4
Jun	86.8	75.5	33.9	2.2	139.6
Jul	67.8	63.1	46.3	5.6	170.1
Aug	50.9	45.3	46.8	0.6	215.8
Sep	49.7	44.0	38.1	2.8	160.8
Oct	59.0	43.5	27.3	5.0	98.4
Nov	50.1	50.5	27.1	0.3	79.6
Dec	53.6	48.9	28.2	0	152.3
Annual	128.6		37.8	31.1	215.8

Source data: *Oltenia Regional Meteorological Center*

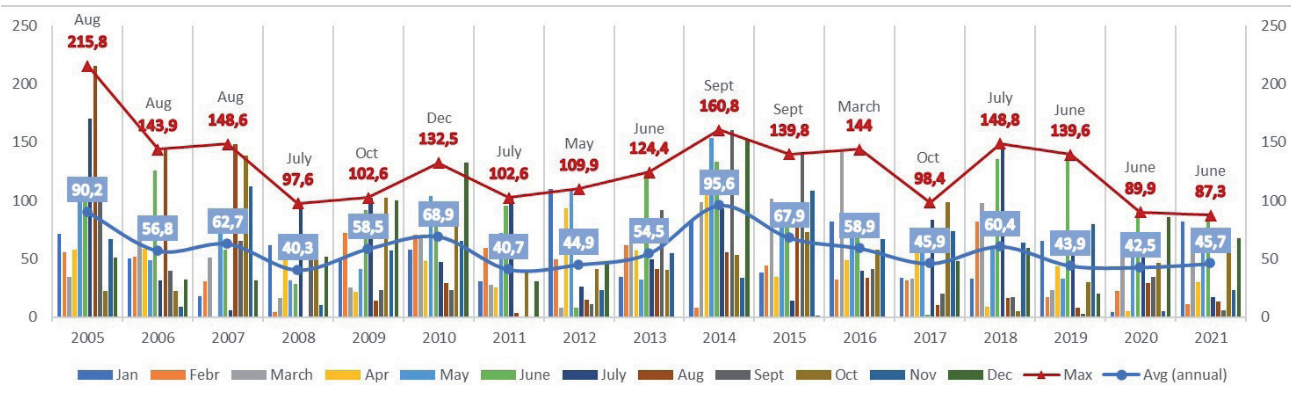

Fig. 5. Means of annual and monthly rainfall data at Craiova meteorological station during 2005-2021.

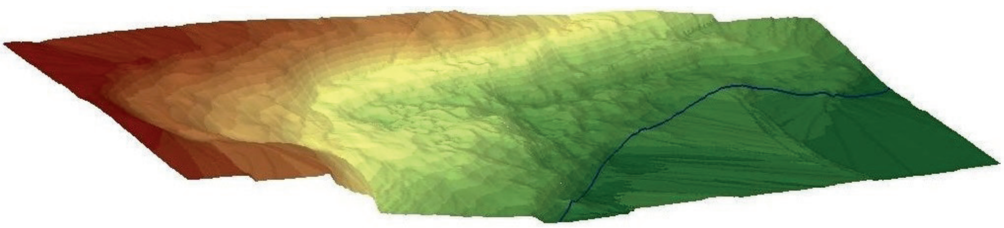

Fig. 6. 3D model of Breasta landslide.

steep, and affected by active collapses. The landslide deposits accumulate at the bottom of the ravine, above the first sliding step. The perimeter of the landslide is 2.23 km, and it affected an area of about 0.3 square kilometers. Its maximum length is 418 m, with a maximum width of 715 m. A Breasta landslide can affect the entire left bank of the Jiu River, reaching the minor bed of its tributary - the Raznic River. In its evolution, the landslide will therefore be influenced by the changes in the litho-structural conditions (consisting of intercalations of sands and clays). In this context, after 2006, extensive sections of the landslide were reactivated due to a significant increase in precipitation, with nearly 500 mm above the annual average of 594.3 mm in 2005.

Fig. 7. Field monitoring – Breasta landslide (2011).

Fig. 8. Reactivation of Breasta landslide (2005 – left; 2011 – right).

What is more significant is that these heavy rainfalls occurred after five consecutive years with precipitation quantities below the annual average. GPS monitoring began in 2006, coinciding with a period of increased precipitation that caused substantial reactivation of the landslide. Subsequent GPS measurements, along the profile line, revealed the most significant morphological changes in the middle and lower sectors of the landslide, where the slope receded by 6 to 19 meters (see Fig. 9). Several depression-like areas, with excess moisture, appeared after the reactivation, partially obstructing the Raznic River channel (see Fig. 10). The continuous instability of the landslide poses a flooding risk for the Breasta settlement. In the event that a larger portion of the landslide becomes active, it could block the course of the Raznic River, resulting in an increase in water levels upstream of the newly formed dam and thus the potential flooding of the Jiu and Raznic Rivers meadows, where the two villages are located.

The topographic model of the landslide surface was created in a GIS environment using terrain measurement data in the ArcGIS software. The DTM for the central

Fig. 9. New scarp of Breasta landslide after the reactivation in 2011.

Fig. 10. Depression-like areas with excessive humidity, after the reactivation in 2011.

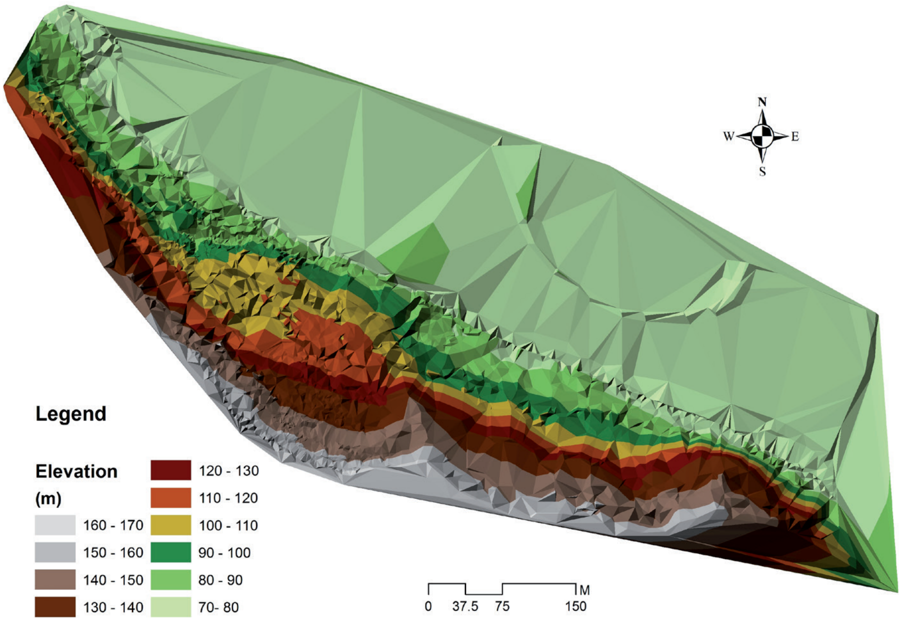

Fig. 11. Breasta landslide – altimetric model (TIN).

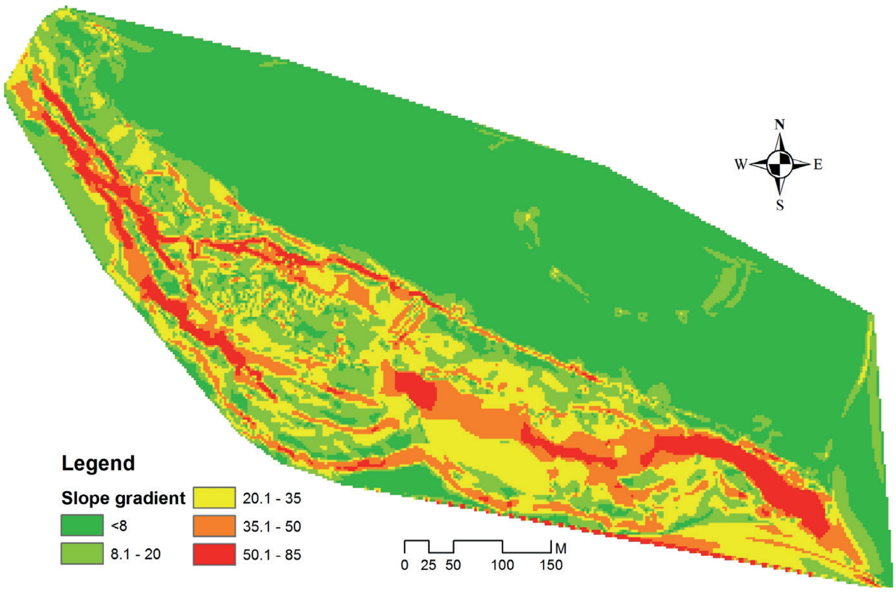

Fig. 12. Breasta landslide – slope map.

sector of the Breasta landslide was generated based on 5000 points collected by the GPS Rover GNSS Smart South S82-T, with a minimum height of 70.5 m and a maximum height of 167.5 m. Using the Kriging method, this sector was enclosed within a rectangle covering an area of 313.390 m^2, with an average height of 108 meters (see Fig. 11). Processing the resulting raster facilitated a surface analysis, including slope angle, slope aspect, and curvature of the landslide (see Fig. 12 and 13). Low-slope surfaces (<8° and 8.1-20°) are characteristic of the floodplain and terraces of the Raznic River, which are generally unaffected by landslides. Moderately inclined surfaces (20.1-35° and 35.1-50°) are more susceptible to mass movements, while highly inclined surfaces (50.1-85°) indicate a high to very high susceptibility to landslides. The reactivation of the slide cannot be attributed only to the inclination of the slopes, but is a combination of factors, to which is also added the geological substrate consisting of intercalations of sands and clays.

The pattern of overall movement on the landslide surface is consistent with field measurements, indicating that the steepest slope gradients (50.1-85°) occur within the western and eastern sectors. Deformation in the western part of the landslide is characterized by nearly vertical slopes. Slope stability analysis conducted using GPS measurements reveals that landslides have occurred along stable and unstable boundaries in saturated

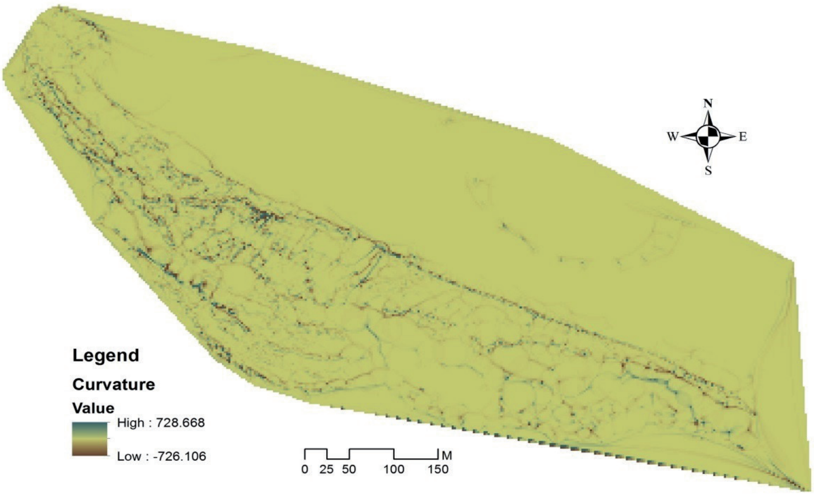

Fig. 13. Breasta landslide– plan curvature map.

conditions (Spring 2011). According to the results, the western and central sectors of the Breasta landslide are the most vulnerable locations. The accuracy of the slope stability assessment was improved with a higher-resolution altimetric model (see Fig. 14 and 15).

Fig. 14. Western sector of Breasta landslide (Spring 2011).

Fig. 15. Central sector of Breasta landslide (Summer 2011).

Areas with pronounced changes in slope and exposure are identified using topographical surface curvature. Values close to zero are assigned to linear surfaces, generally associated with low declivity slopes. Maximum positive values indicate surfaces with a high to very high probability of mass movement occurrence (see Fig. 13), with data being validated in the field in the spring and summer seasons of 2006 and 2011.

Discussion

The research continues previous work done on the landslides in the Piedmont area of Romania. Here we propose a new analysis based on GNNS measurements and the GIS approach. This is profiting both from expert knowledge and field research. Limitations deriving from the landslide inventories are related to their incompleteness, spatial heterogeneity, and location inaccuracies. The limitations deriving from the Breasta landslide monitoring are related to the incompleteness and spatial heterogeneity of point measurements. Under these circumstances, the insertion of motion sensors at the level of unstable areas is considered an adequate analysis method. Future efforts regarding the mapping of the Breasta landslide aim at correlating the restored areas with local natural factors and social vulnerability.

Consequently, the reactivation of certain sections of the Breasta landslide could pose a real threat to the Breasta settlements. The obstruction of the Raznic River, coupled with a significant flood, could have devastating effects on these settlements as well as the nearby arable lands (see Fig. 14 and 15). This aspect should be better accounted for in the future by implementing several measures to mitigate and prevent landslides:

– Drainage of the accumulated water from the landslide area;
– Afforestation of the slope, especially in the reactivated section;
– Restricting grazing in the area;

– Raising the protective dam along the Jiu River and extending the dam on the Raznic River;
– Informing the residents in the area about the potential flood danger and the necessary measures to take in case of flooding.

Conclusions

This study examines the behavior of a landslide located on the right bank of the Jiu River in southwestern Romania. The 16-year monitoring data set (2006–2022) contributes to a better understanding of surface movement. By correlating morphological observations with climatic and geological data, it is observed that the most intense movements occurred in years with above-average precipitation, especially when they followed dry years.

Some limitations of the approach and, hence, of the output maps derive from the spatial and temporal heterogeneity of the landslide databases. Our study shows that, in order to increase the accuracy of results, a more enhanced geodatabase of the Breasta landslide reactivation areas assessment according to triggering factors. This could be achieved through advanced monitoring through field research campaigns and remote sensing applications.

In spite of the uncertainties inherent to landslide mapping and monitoring, it can be concluded that the research results can support territorial planning and civil protection plans. We thus consider that the methodological frameworks used in our study can be applied to other Piedmont regions to produce geomorphological maps for territorial planning, land use, tourism, and conservation purposes.

Future investigations and instrumentation should be expanded based on the current data, the significance of the study area, and the confirmed geomorphic activities. Finally, the landslide maps generated by this study can serve as effective tools for future land planning and monitoring by government officials, research experts, and scholars.

Acknowledgments

Daniel Simulescu, Oana Mititelu-Ionuș, Sandu Boengiu, Cristiana Vîlcea, Mirela Mazilu, Simona Mariana Popescu and Emil Marinescu thank the University of Craiova for their scientific and technical support. Valentina Nikolova acknowledges the project BG05M2OP001-2.016-0022 Modernization of higher education in sustainable use of natural resources in Bulgaria – NATURESEDU. The authors are grateful to the Oltenia Regional Meteorological Center for providing the rainfall data used for the present analysis.

Conflict of Interest

Authors declare no conflict of interest.

References

1. ESCOBAR-WOLF R., SANDERS J.D., VISHNU C.L., OOMMEN T., SAJINKUMAR K.S. A GIS tool for infinite slope stability analysis (GIS-TISSA). Geoscience Frontiers, **12** (2), 756, **2021**.
2. PHAM B.T., TIEN BUI D., PRAKASH I. Bagging based support vector machines for spatial prediction of landslides. Environmental Earth Sciences, **77**, 146, **2018**.
3. KYRIOU A., NIKOLAKOPOULOS K., KOUKOUVELAS I., LAMPROPOULOU P. Repeated UAV campaigns, GNSS measurements, GIS, and petrographic analyses for landslide mapping and monitoring. Minerals, **11** (3), 300, **2021**.
4. XIE M., ZHAO W., JU N., HE C., HUANG H., CUI Q. Landslide evolution assessment based on InSAR and real-time monitoring of a large reactivated landslide. Wenchuan, China. Engineering Geology, **277**, 105781, **2020**.
5. FRODELLA W., CIAMPALINI A., BARDI F., SALVATICI T., DI TRAGLIA F., BASILE G., CASAGLI N. A method for assessing and managing landslide residual hazard in urban areas. Landslides, **15**, 183, **2018**.
6. CARLÀ T., INTRIERI E., DI TRAGLIA F., NOLESINI T., GIGLI G., CASAGLI N. Guidelines on the use of inverse velocity method as a tool for setting alarm thresholds and forecasting landslides and structure collapses. Landslides, **14,** 517, **2017**.
7. LOMBARDI L., NOCENTINI M., FRODELLA W., NOLESINI T., BARDI F., INTRIERI E., CARLA T., SOLARI L., DOTTA G., FERRIGNO F. The Calatabiano landslide (southern Italy): Preliminary GB-InSAR monitoring data and remote 3D mapping. Landslides, **14,** 685, **2017**.
8. RASPINI F., BIANCHINI S., CIAMPALINI A., DEL SOLDATO M., MONTALTI R., SOLARI L., TOFANI V., CASAGLI N. Persistent Scatterers continuous streaming for landslide monitoring and mapping: The case of the Tuscany region (Italy). Landslides, **16,** 2033, **2019**.
9. NIKOLOVA V., KAMBUROV A. Geoinformation technologies in the evaluation of short-term geomorphic change: An example of Damdere debris flood area (Bulgaria). Journal of the Geographical Institute "Jovan Cvijić" SASA, **72** (2), 133, **2022**.
10. VAN WESTEN CJ., CASTELLANOS E., KURIAKOSE SL. Spatial data for landslide susceptibility, hazard, and vulnerability assessment: an overview. Engineering Geology, **102** (3-4), 112, **2008**.
11. CHAE B.G., PARK H.J., CATANI F., SIMONI A., BERTI M. Landslide prediction, moni-toring and early warning: a concise review of state-of-the-art. Geosciences Journal, **21** (6), 1033, **2017**.
12. JI J., CUI H., ZHANG T., SONG J., GAO Y. A GIS-based tool for probabilistic physical modelling and prediction of landslides: GIS-FORM landslide susceptibility analysis in seismic areas. Landslides, **19** (9), 2213, **2022**.
13. FAN R., ZHOU X., TIAN F., TANG Y., YIN L., XIANG J. GIS-Based Landslide Susceptibility Zonation Mapping Using the Weighted Information Model in Erlang Mountain-Zheduo Mountain Power Transmission Project,

China. Polish Journal of Environmental Studies, **33** (1), 609, **2023**.
14. MEDINA V., HÜRLIMANN M., GUO Z., LLORET A., VAUNA, J. Fast physically-based model for rainfall-induced landslide susceptibility assessment at regional scale. Catena, **201**, 105213, **2021**.
15. MA S., SHAO X., XU C. Characterizing the Distribution Pattern and a Physically Based Susceptibility Assessment of Shallow Landslides Triggered by the 2019 Heavy Rainfall Event in Longchuan County, Guangdong Province, China. Remote Sensing, **14** (17), 4257, **2022**.
16. SIM K.B., LEE M.L., WONG S.Y. A review of landslide acceptable risk and tolerable risk. Geoenvironmental Disasters, **9** (1), 3, **2022**.
17. CASAGLI N., INTRIERI E., TOFANI V., GIGLI G., RASPINI F. Landslide detection, monitoring and prediction with remote-sensing techniques. Nature Reviews Earth & Environment, **4** (1), 51, **2023**.
18. DUMITRAȘCU M., DRAGOTĂ C.S., GRIGORESCU I., DUMITRAŞCU C., VLĂDUŢ A. Key pluvial parameters in assessing rainfall erosivity in the south-west development region, Romania. Journal of Earth System Science, **126** (1), 1, **2017**.
19. MINEA G., IOANA-TOROIMAC G., MOROȘANU G. The dominant runoff processes on grassland versus bare soil hillslopes in a temperate environment-An experimental study. Journal of Hydrology and Hydromechanics, **67** (4), 297, **2019**.
20. NICULIŢĂ M., MĂRGĂRINT M.C., SANTANGELO M. Archaeological evidence for Holocene landslide activity in the Eastern Carpathian lowland. Quaternary International, **415** (1), 175, **2016**.
21. MICU M., JURCHESCU M.S., SANDRIC I., MARGARINT M.C., CHITU Z., MICU D., CIUREAN R., ILINCA V., VASILE M. Mass Movements. In Radoane M., Vespremeanu-Stroe A., Eds. Landform Dynamics and Evolution in Romania, Springer International Publishing: Cham, Switzerland, pp. 765, **2017**.
22. BĂLTEANU D., MICU M., JURCHESCU M., MALET J-P., SIMA M., KUCSICSA G., DUMITRICĂ C., PETREA D., MĂRGĂRINT M.C., BILAȘCO S., DOBRESCU C.F., CĂLĂRAȘU E.-A., OLINIC E., BOȚI I., SENZACONI F. National-Scale Landslide Susceptibility Map of Romania in a European Methodological Framework. Geomorphology, **371**, 107432, **2020**.
23. GROZAVU A., PATRICHE C. Mapping Landslide Susceptibility at National Scale by Spatial Multi-Criteria Evaluation, Geomat. Nat. Hazards Risks, **12**, 1127, **2021**.
24. BOENGIU S., IONUȘ O., SIMULESCU D., POPESCU L. River undercutting and induced landslide hazard. The Jiu Rivervalley (Romania) as a case study. Geomorphologia Slovaca et Bohemica, **2**, 46, **2011**.
25. PALIS E., LEBOURG T., TRIC E., MALET J.P., VIDAL M. Long-term monitoring of a large deepseated landslide (La Clapiere, South-East French Alps): initial study. Landslides, **14** (1), 155, **2017**.
26. CHEN W., POURGHASEMI H.R., NAGHIBI S.A. Prioritization of landslide conditioning factors and its spatial modeling in Shangnan County, China using GIS-based data mining algorithms. Bulletin of Engineering Geology and the Environment, **77** (1), 611, **2018**.
27. MCCOLL S.T. Landslide causes and triggers. In Landslide hazards, risks, and disasters, Second Edition, Tim Davies, Nick Rosser and J.F. Shroder Editors, pp. 13, **2021**. Elsevier.
28. SESTRAS P., BILAȘCO Ș., ROȘCA S., VERES I., ILIES N., HYSA A., SPALEVIC V., CÎMPEANU S.M. Multi-Instrumental Approach to Slope Failure Monitoring in a Landslide Susceptible Newly Built-Up Area: Topo-Geodetic Survey. UAV 3D Modelling and Ground-Penetrating Radar. Remote Sensing, **14** (22), 5822, **2022**.
29. BOUALI E.H., OOMMEN T., ESCOBAR-WOLF R. Evidence of instability in previously-mapped landslides as measured using GPS, optical, and SAR data between 2007 and 2017: a case study in the Portuguese Bend landslide complex, California. Remote Sensing, **11** (8), 937, **2019**.
30. ZULIANI D., TUNINI L., DI TRAGLIA F., CHERSICH M., CURONE D. Cost-effective, single-frequency GPS network as a tool for landslide monitoring. Sensors, **22** (9), 3526, **2022**.
31. BUNN M., LESHCHINSKY B., OLSEN M.J. Estimates of three-dimensional rupture surface geometry of deep-seated landslides using landslide inventories and high-resolution topographic data. Geomorphology, **367**, 107332, **2020**.
32. CHANDLER B.M., LOVELL H., BOSTON C.M., LUKAS S., BARR I.D., BENEDIKTSSON ÍÖ, BENN D.I., CLARK C.D., DARVILL C.M., EVANS D.J.A., EWERTOWSKI M.W., LOIBL D., MARGOLD M., OTTO J.-C., ROBERTS D.H., STOKES C.R., STORRAR R.D., STROEVEN AP. Glacial geomorphological mapping: A review of approaches and frameworks for best practice. Earth-Science Reviews, **185**, 806, **2018**.
33. VOJTEKOVÁ J., VOJTEK M. Assessment of landslide susceptibility at a local spatial scale applying the multi-criteria analysis and GIS: a case study from Slovakia. Geomatics. Natural Hazards and Risk, **11** (1), 131, **2020**.
34. CAMPOS N., QUESADA-ROMÁN A., GRANADOS-BOLAÑOS S. Mapping Mountain Landforms and Its Dynamics: Study Cases in Tropical Environment. Applied Sciences, **12** (21), 10843, **2022**.
35. HARMOUZI H., SCHLÖGEL R., JURCHESCU M., HAVENITH H.B. Landslide susceptibility mapping in the Vrancea-Buzău seismic region, southeast Romania. Geosciences, **11** (12), 495, **2021**.
36. OTTO J.C., PRASICEK G., BLÖTHE J., SCHROTT L. GIS Applications in geomorphology. Comprehensive Geographic Information Systems, **1**, 81, **2018**.
37. BROCK J., SCHRATZ P., PETSCHKO H., MUENCHOW J., MICU M., BRENNING A. The performance of landslide susceptibility models critically depends on the quality of digital elevation models. Geomatics, Natural Hazards and Risk, **11** (11), 1075, **2020**.
38. BOENGIU S., VLADUT A., MARINESCU E. Conditions of gully development within piedmont areas with examples from the western part of the Getic Piedmont, Romania. Journal of Environmental Biology, **33** (2), 407, **2012**.
39. SABĂU D.A., ȘERBAN G., BREŢCAN P., DUNEA D., PETREA D., RUS I., TANISLAV D. Combining radar quantitative precipitation estimates (QPEs) with distributed hydrological model for controlling transit of flash-flood upstream of crowded human habitats in Romania. Natural Hazards, **116** (1), 1209, **2023**.